*Journal of The Electrochemical Society*, **149** (5) C237-C243 (2002)
0013-4651/2002/149(5)/C237/7/$7.00 © The Electrochemical Society, Inc.

# Effects of TaN Substrate Pretreatment by Ar Plasma on Copper Chemical Vapor Deposition

**Cheng-Li Lin,[z] Peng-Sen Chen, and Mao-Chieh Chen***

*Department of Electronics Engineering and Institute of Electronics, National Chiao-Tung University, Hsinchu 300, Taiwan*

CVD Cu films deposited on TaN substrates with and without an Ar plasma treatment prior to Cu film deposition and the effects of postdeposition thermal annealing were investigated. Cu films deposited on an Ar-plasma-treated TaN substrate have a number of favorable properties over the films deposited on a TaN substrate without the plasma treatment. These include a smoother film surface, regular arrangement of Cu grains, and increased (111)-preferred orientation. The postdeposition thermal annealing enhanced the (111)-preferred orientation and decreased the resistivity of the as-deposited Cu films. As the results of Ar plasma substrate pretreatment, we presume that the smoother and amorphous-like surface layer of the TaN substrate enhanced the formation of the most stable (111) texture Cu films, and that the higher substrate surface energy resulted in Cu films with smoother surface and regularly shaped smaller grains. Thus, a combined process including Ar plasma substrate treatment prior to Cu film deposition and postdeposition thermal annealing at an appropriate temperature in $N_2$ ambient is proposed for the advantages of low-resistivity and high (111)-oriented Cu film deposition.
© 2002 The Electrochemical Society. [DOI: 10.1149/1.1462794] All rights reserved.

Manuscript submitted June 26, 2001; revised manuscript received November 22, 2001. Available electronically March 20, 2002.

As integrated circuits advance into deep sub-quarter-micrometer regime, the conventional Al-based interconnect scheme is faced with various performance and reliability challenges, such as interconnect propagation delay and the problem of electromigration.[1,2] Therefore, other metals with a lower electrical resistivity and superior electromigration resistance are needed to replace Al as the interconnect material. Copper has been regarded as a potential candidate to replace Al and its alloys for multilevel interconnection applications because of its low bulk resistivity (1.67 $\mu\Omega$ cm), excellent electromigration resistance, and high resistance to stress-induced voids.[3,4] There are various techniques for copper film deposition, such as chemical vapor deposition (CVD),[5,6] conventional as well as ionized metal plasma (IMP), physical vapor deposition (PVD),[7] and electrochemical deposition (ECD) including electroplating and electroless plating;[8,9] among these, the CVD method has the advantages of superior step coverage and excellent gap-filling capability for high-aspect-ratio vias and trenches,[6] making it the most promising Cu film deposition technique for future integrated circuit (IC) applications. Since it is difficult to pattern the Cu film by dry etch methods, the Cu damascene process is developed to cope with this difficulty. The dual damascene process on scaled-down devices requires perfect gap-filling capability of copper for high-aspect-ratio vias and trenches. Although the Cu ECD combined with IMP of a thin Cu seed layer and barrier layers provides a suitable solution for IC technologies above 0.25 $\mu$m, deposition techniques for a conformal and continuous thin barrier as well as a conformal and void-free Cu film filling into deep sub-quarter-micrometer vias, such as CVD, are eventually unavoidable for future-generation devices.[10] A number of barrier materials have been used as substrates for CVD of Cu films, such as W, Ti, TiN, Ta, and TaN;[5,11-13] among them, TaN exhibits a superb barrier capability against Cu diffusion.[14] However, the chemically vapor-deposited Cu films on TaN substrate exhibited a fairly low-peak-ratio of Cu(111)/Cu(200) preferred orientation in the X-ray diffraction (XRD) spectrum,[5,13] which is unfavorable for electromigration resistance. Since the nucleation process and the microstructure of Cu films are very sensitive to the substrate surface conditions,[15,16] it has been reported that plasma treatment on the substrate surface prior to the Cu film deposition results in deposited films with preferred (111) texture.[17,18]

In this work, effects of TaN substrate pretreatment by Ar plasma on copper CVD were investigated using a multichamber low-pressure CVD system. The effects of postdeposition thermal annealing were also investigated.

## Experimental

Figure 1 shows a schematic of the multichamber Cu CVD apparatus built for this study. The apparatus consists of a cluster of four chambers and a direct liquid injection (DLI) system for precursor delivery. The chamber cluster is composed of a sample-loading chamber (for samples loading/unloading), a pretreatment chamber, a reaction chamber, and a transfer chamber. The pretreatment chamber is used to preclean and/or modify the substrate surface by plasma treatment. CVD of Cu films is to be carried out in the reaction chamber. The transfer chamber, which houses a robot arm, is designed to handle the transfer of a sample to and from each chamber. In the reaction chamber there is a shower-head injector through which the Cu precursor is introduced into the reaction chamber in a stream of carrier gas. Under the injector, there is a substrate susceptor that can be heated by a resistive heating element up to a maximum temperature of 400°C. The susceptor is also rotatable for better uniformity of film deposition. The shower-head injector is moveable in the vertical direction so that the distance between the injector and the sample can be adjusted. The sidewall of the reaction chamber and the precursor injector are kept at a temperature of 45°C by the circulation of warm water to prevent Cu deposition of precursor condensation.

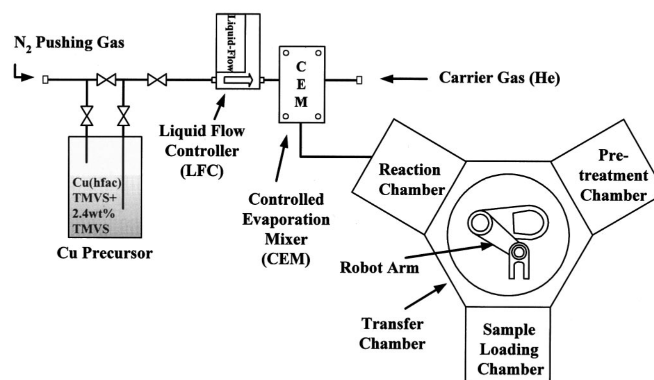


**Figure 1.** Schematic of multichamber Cu CVD apparatus built for this study.

* Electrochemical Society Active Member.
[z] E-mail address: cllin.ee85g@nctu.edu.tw

Downloaded on 2014-04-27 to IP 140.113.38.11 address. Redistribution subject to ECS terms of use (see ecsdl.org/site/terms_use) unless CC License in place (see abstract).

**Table I. Processing conditions for multichamber Cu CVD system.**

| Pretreatment chamber (Ar plasma operating conditions) | | Reaction chamber (Cu film deposition conditions) | |
|---|---|---|---|
| Substrate temperature (°C) | 80 | Substrate temperature (°C) | 120-240 |
| Operating pressure (mTorr) | 40 | Operating pressure (mTorr) | 150 |
| Ar gas flow rate (sccm) | 6 | Cu precursor flow rate (mL/min) | 0.4 |
| RF power (W) | 50 | CEM temperature (°C) | 70 |
| Self-dc bias (V) | −270 | Carrier gas (He) flow rate (sccm) | 25 |
| Pretreatment time (min) | 10 | Substrate holder rotation speed (rpm) | 10 |
| | | Gas-injector/susceptor distance (cm) | 2 |
| | | Delivery line temperature (°C) | 72 |
| | | Reactor wall temperature (°C) | 45 |

The Cu precursor used in this study is Cu(1,1,1,5,5,5-hexafluoroacetylacetonate)trimethylvinylsilane [Cu(hfac)TMVS] with 2.4 wt % TMVS additive.[19-21] The 2.4 wt % TMVS enhances the stability of the precursor.[21] The liquid Cu precursor is delivered by the DLI system consisting of a liquid flow controller (LFC) and a controlled evaporation mixer (CEM) (Fig. 1). Initially, the liquid precursor is propelled by $N_2$ gas through the LFC. It is then vaporized in the CEM and mixed with the carrier gas. Helium (He) is used as the carrier gas in this study. The precursor-saturated carrier gas is introduced into the reaction chamber through the gas injector.

In this work, TaN was used as the substrate for the CVD of Cu films. TaN layers of 50 nm thickness were sputter-deposited on a thermal-oxide (500 nm thickness)-covered Si wafer. A dc magnetron sputtering system with a base pressure of $1.5 \times 10^{-6}$ Torr was used to reactively sputter a Ta target (99.99% purity) in an $Ar/N_2$ gas mixture at a pressure of 7.6 mTorr for TaN film deposition. The flow rates of Ar and $N_2$ were 24 and 6 sccm, respectively, for making the gas mixture, and the TaN films were sputter-deposited at a power of 150 W. The TaN-coated substrate wafer was loaded into the multichamber Cu CVD system. When the pressure of the sample-loading chamber reached $10^{-6}$ Torr, the substrate wafer (together with the substrate holder) was transferred to the pretreatment chamber or reaction chamber via the transfer chamber depending on the process requirement of whether the plasma pretreatment on substrate was to be performed or not. In this study, Ar plasma treatment was performed at 50 W power for 10 min under the following conditions: Ar flow rate 6 sccm, gas pressure 40 mTorr, substrate temperature 80°C, and self-dc bias −270 V. After the plasma pretreatment, the sample was transferred to the reaction chamber for Cu film deposition. Prior to Cu film deposition, the substrate sample was heated to the desired deposition temperature with He carrier gas flowing at 25 sccm and the chamber pressure maintained at 150 mTorr. Usually, approximately 1 h is required for the substrate sample to reach the preset temperature. In this study, Cu CVD was performed over a temperature range of 120-240°C at a pressure of 150 mTorr with a precursor flow rate of 0.4 mL/min and a He carrier gas flow rate of 25 sccm. Major processing conditions and the parameters of the Cu CVD system used in this study are summarized in Table I. At the end of Cu film deposition, the sample was cooled in the ambient of He at a pressure of 150 mTorr.

The thickness of Cu films was measured using a DekTek profiler on the patterned Cu films and was verified by cross-sectional scanning electron microscopy (SEM). SEM was also used to observe the surface morphology of the deposited Cu films and cross-sectional views of copper nucleated on TaN substrate. A four-point probe was employed to measure the sheet resistance. Auger electron spectroscopy (AES) was used to analyze the impurity content in the Cu films. The crystal structure was identified by XRD analysis. The surface roughnesses of the Cu and substrate TaN films were evaluated by atomic force microscopy (AFM). Rutherford backscattering spectroscopy (RBS) was used to determine the composition of the TaN substrate samples.

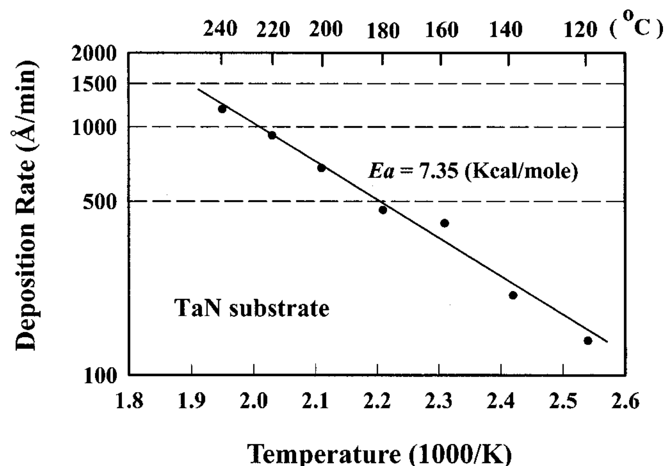


**Figure 2.** Deposition rate *vs.* substrate temperature (Arrhenius plot) at a constant pressure of 150 mTorr for TaN substrate.

## Results and Discussion

*CVD Cu films on TaN substrates.*—Cu films were chemically vapor deposited on reactively sputtered TaN substrates, which have a resistivity of 0.6 mΩ cm and a composition of $TaN_{1.2}$, as determined by RBS. Figure 2 shows the deposition rate of Cu films as a function of substrate temperature (Arrhenius plot) at a constant pressure of 150 mTorr with a He carrier gas flow rate of 25 sccm and a liquid Cu precursor flow rate of 0.4 mL/min. Since the chemical reaction of Cu CVD involves basically a thermal dissociation of the Cu precursor, a higher temperature would result in a higher rate of deposition. The activaton energy $E_a$ was determined to be 7.35 kcal/mol by the Arrhenius equation

$$R = R_0 \exp(-E_a/kT) \quad [1]$$

where $R$ is the deposition rate, $R_0$ is the Arrhenius pre-exponential constant or frequency factor, $k$ is the Boltzmann constant, and $T$ is the absolute temperature. Other values of activation energy were reported in the literature, *e.g.*, the values of 10.20 kcal/mol (deposited on W substrates at 0.5 Torr),[22] 16.70 kcal/mol (deposited on TiN substrates at 10.5 Torr),[23] 19.30 kcal/mol (deposited on Ta substrates at 1.5 Torr),[5] and 17.90 kcal/mol (deposited on TiN substrates at 0.5 Torr).[21] The difference in the values of the activation energy is presumably due to different deposition conditions.

The SEM micrographs in Fig. 3 show the surface morphology of copper films deposited at various temperatures for a deposition time of 10 min. The grain size of Cu increases with the deposition temperature. At higher deposition temperatures (200-240°C), the Cu films exhibit stacked grains featuring clear boundaries as well as voids between large grains. Figure 4 shows the grain size of Cu increasing with the deposition temperature. The resistivity of Cu films was calculated using the measured sheet resistances and film thicknesses. Figure 5 illustrates the resistivity of Cu films as a function of deposition temperature at a deposition pressure of 150 mTorr. It has been reported that the resistivity of CVD Cu films is closely related with the impurity content and microstructure.[24,25] The slightly higher resistivity at low deposition temperatures is presum-

Downloaded on 2014-04-27 to IP 140.113.38.11 address. Redistribution subject to ECS terms of use (see ecsdl.org/site/terms_use) unless CC License in place (see abstract).

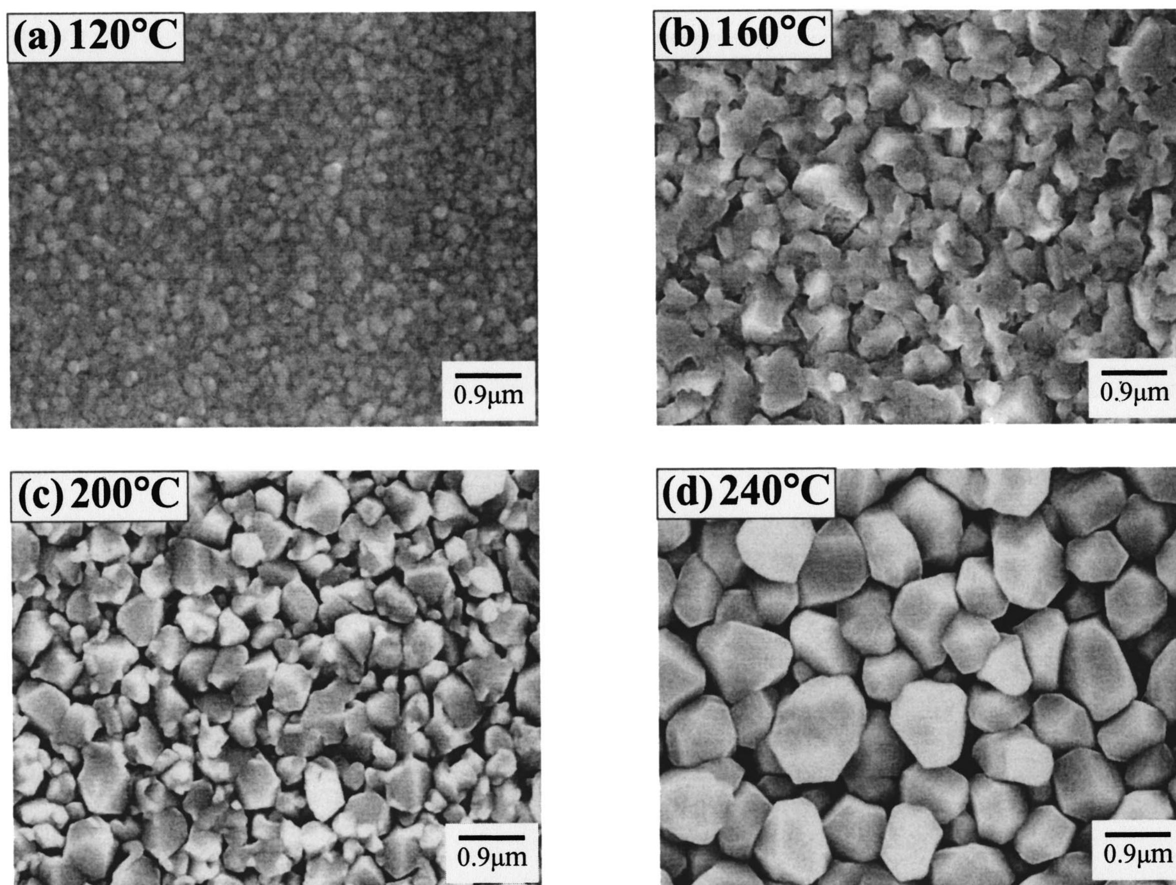


**Figure 3.** SEM micrographs showing surface morphology of Cu films deposited on TaN substrates at temperatures of (a) 120, (b) 160, (c) 200, and (d) 240°C. The films were deposited at a constant pressure of 150 mTorr for 10 min.

ably due to higher contamination of residual impurities from the reaction by-products, while the high resistivity at high deposition temperatures results from the higher contamination of impurities in the film as well as the porous film structure. The most appropriate temperature for Cu film deposition from the viewpoint of low resistivity under the present deposition condition appears to be around 160°C (2.30 $\mu\Omega$ cm). Figure 6 illustrates the AES depth profiles of CVD Cu films deposited on TaN substrates. The most notable impurities contaminated in CVD Cu films are carbon (C) and oxygen (O), which may result from incomplete desorption of hfac ligand during the CVD process.[25]

*Nucleation and surface morphology observation.*—The surface conditions of substrates play an important role in the CVD of Cu films. Figure 7 shows AFM images of the TaN substrate before and after Ar plasma treatment at 50 W for 10 min. The Ar plasma treat-

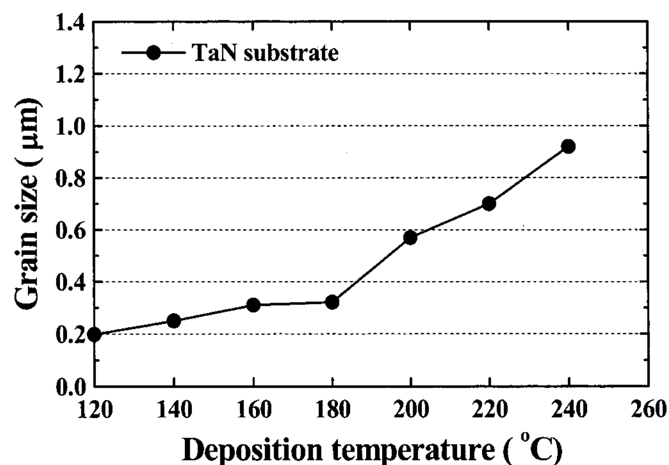


**Figure 4.** Grain size *vs.* deposition temperature for Cu films deposited at a constant pressure of 150 mTorr for 10 min.

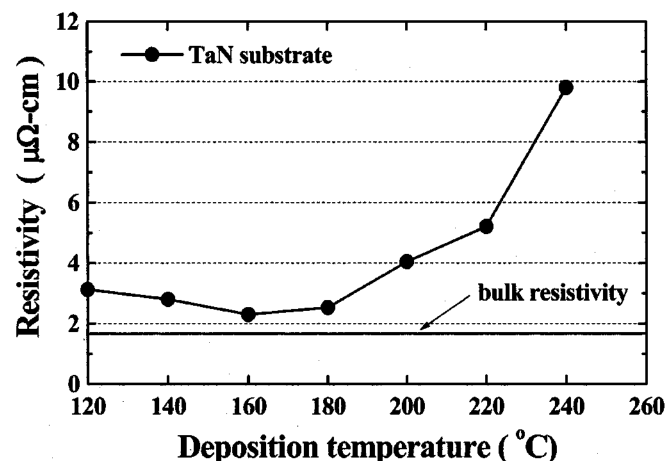


**Figure 5.** Resistivity of Cu film *vs.* deposition temperature for Cu films deposited at a constant pressure of 150 mTorr.

Downloaded on 2014-04-27 to IP 140.113.38.11 address. Redistribution subject to ECS terms of use (see ecsdl.org/site/terms_use) unless CC License in place (see abstract).

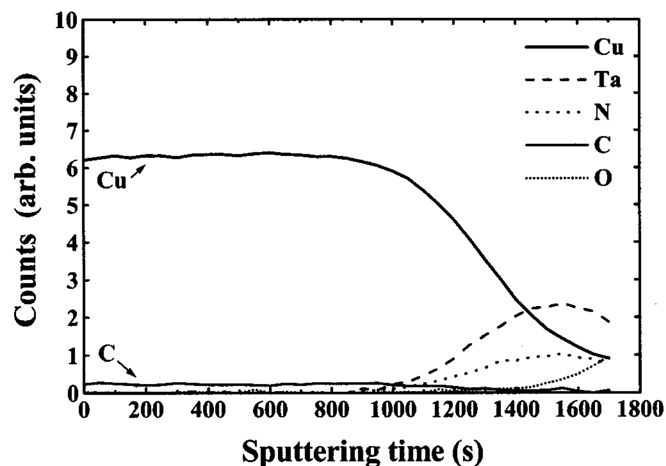


**Figure 6.** AES depth profiles of Cu films deposited on TaN substrates (without plasma treatment prior to Cu deposition).

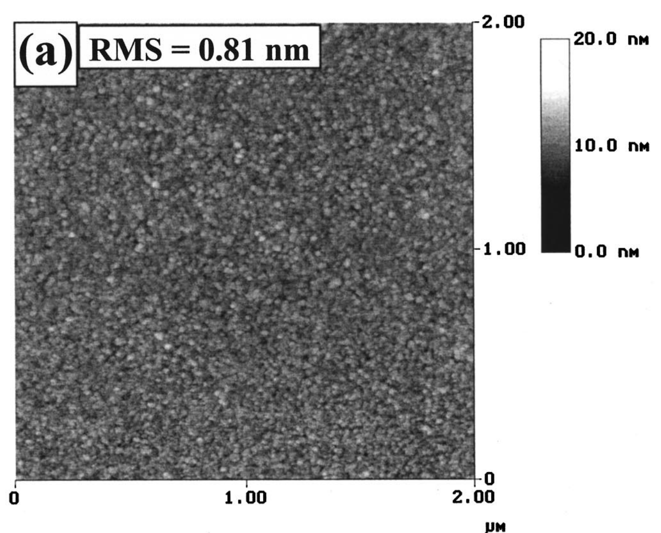


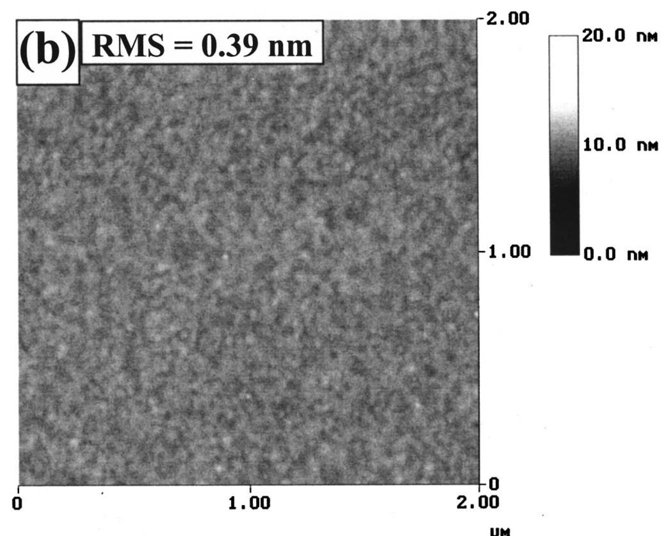


**Figure 7.** AFM images showing surface morphology of TaN substrates (a) without plasma treatment and (b) with Ar plasma treatment (at 50 W with 40 mTorr pressure for a plasma time of 10 min).

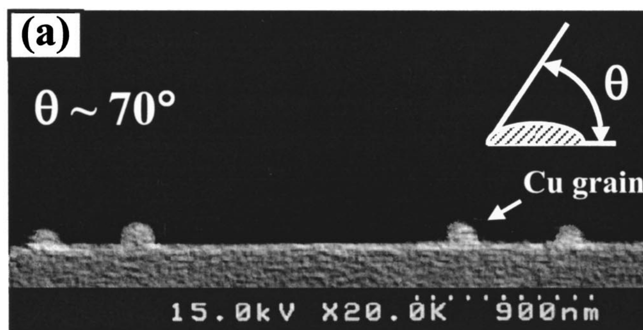


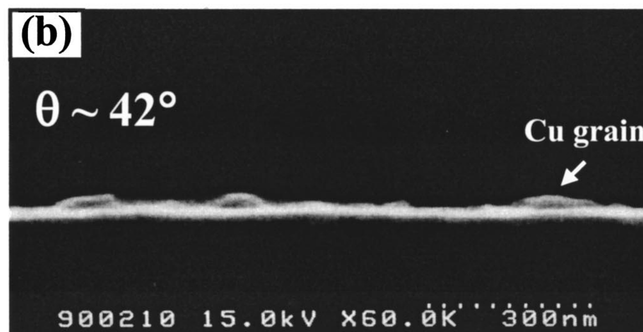


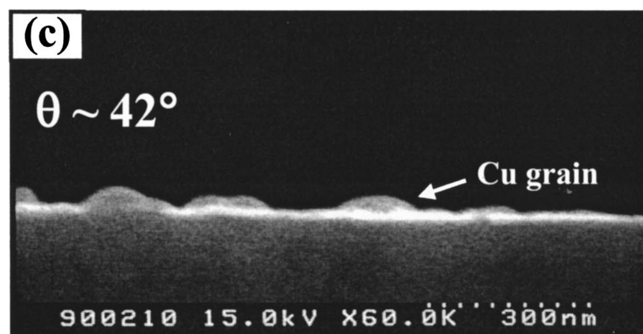


**Figure 8.** SEM micrographs showing cross-sectional view of copper grains on TaN substrates: (a) without plasma treatment (after 1 min deposition time), (b) with Ar plasma treatment (after 1 min deposition time), and (c) with Ar plasma treatment (after 2 min deposition time).

ment significantly improved the surface smoothness of the TaN substrate. In order to study the effect of substrate pretreatment by Ar plasma, the nucleation process of Cu films was investigated. Figure 8 illustrates the cross-sectional view SEM micrographs for Cu nucleation on TaN substrates with and without an Ar plasma treatment. On a TaN substrate without Ar plasma treatment, the initial 1 min deposition resulted in Cu grains of spherical shape with a wetting angle (contact angle) of about 70° (Fig. 8a), similar to Al nucleation on TiN substrates reported in the literature.[26] On the Ar-plasma-treated TaN substrate, the Cu grains show a flat-dome shape with a wetting angle of about 42° (Fig. 8b); after 2 min deposition, the grains grew and became larger in size, but the grain shape remained basically unchanged (Fig. 8c). According to Young's equation[18,27]

$$\cos\theta = \frac{\sigma_s - \sigma_i}{\sigma_c} \quad [2]$$

where $\theta$ is the wetting angle (contact angle) of the copper grain, $\sigma_s$ and $\sigma_c$ are the respective surface energy of the TaN substrate and the Cu grain, and $\sigma_i$ is the interfacial energy between the Cu grain and the TaN substrate. The smaller wetting angle of 42° indicates that the Ar-plasma-treated TaN substrate has a higher substrate surface

Downloaded on 2014-04-27 to IP 140.113.38.11 address. Redistribution subject to ECS terms of use (see ecsdl.org/site/terms_use) unless CC License in place (see abstract).

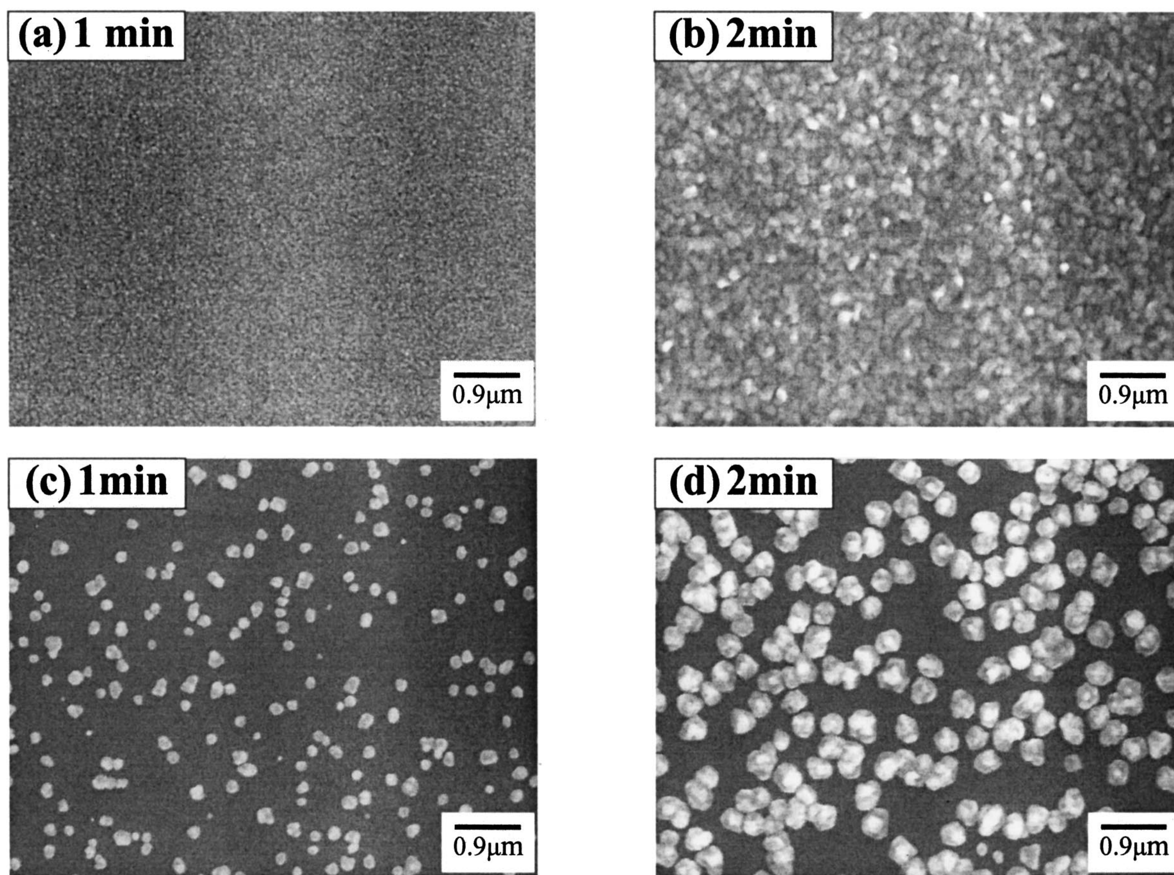


**Figure 9.** SEM micrographs showing Cu nucleation at 160°C for (a) 1 and (b) 2 min deposition on TaN substrate with Ar plasma treatment, and (c) 1 and (d) 2 min deposition on TaN substrate without plasma treatment.

energy or lower interfacial energy, thus enhancing the Cu films growth by two dimensions (layer growth) and forming the most stable (111) closely packed configuration.[18,28] Moreover, the Cu-containing adspecies tend to nucleate uniformly on the Ar-plasma-treated TaN substrate. A similar result was reported for the CVD Al nucleation on a $SiO_2$-coated substrate pretreated by $H_2$ plasma.[29] Figure 9 shows top-view SEM micrographs for the nucleation process of Cu films deposited at 160°C on a TaN substrate with and without an Ar plasma treatment. On the Ar-plasma-treated TaN substrate, the Cu-containing adspecies [Cu(hfac)] easily and uniformly nucleated on the substrate surface, forming dense and small Cu nuclei after 1 min deposition (Fig. 9a). The Cu-containing adspecies continuously adsorbed on the surface of Cu nuclei to proceed with the growth of copper nuclei, resulting in larger Cu grains and a continuous Cu film after 2 min deposition (Fig. 9b). On the TaN substrate without Ar plasma treatment, the Cu-containing adspecies were sparsely nucleated on the substrate surface, and the subsequent adspecies tend to nucleate on the existing Cu nuclei rather than the TaN substrate. As a result, the Cu nuclei grew into Cu grains sparsely distributed on the substrate, while a few new Cu nuclei also randomly nucleated directly on the TaN substrate, forming smaller Cu grains (Fig. 9c). After 2 min deposition, all grains grew larger, though a few new smaller grains are scattered among the larger ones (Fig. 9d). A similar result was reported in the literature that the nucleation of Cu on the $H_2$-plasma-treated TiN substrate led to a dense distribution of Cu grains.[30] The SEM micrograph in Fig. 10 shows the surface morphology of a Cu film deposited at 160°C for 10 min on the Ar-plasma-treated TaN substrate. In comparison with the corresponding Cu film deposited on the TaN substrate without Ar plasma treatment (Fig. 3b), the surface morphology of the Cu film deposited on the Ar-plasma-treated TaN substrate reveals regularly shaped smaller grains. As a result, better surface smoothness is expected for the Cu film deposited on the Ar-plasma-treated TaN substrate. This is evidenced by the results of AFM analysis shown in Fig. 11. The Cu film deposited on the TaN substrate without Ar plasma treatment shows irregular Cu grains with an average surface roughness [root-mean-square (rms)] of 55.9 nm, while the Cu film deposited on the Ar-plasma-treated TaN substrate shows much regular and smaller grains with an average surface roughness (rms) of 32.8 nm.

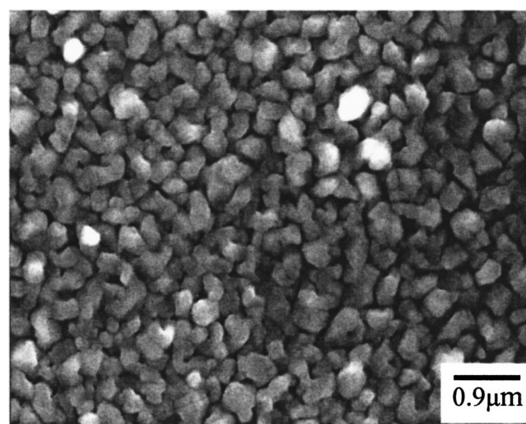


**Figure 10.** SEM micrographs showing surface morphology of Cu film deposited on TaN substrate with Ar plasma treatment prior to Cu deposition. The Cu film was deposited at 160°C and 150 mTorr for 10 min.

Downloaded on 2014-04-27 to IP 140.113.38.11 address. Redistribution subject to ECS terms of use (see ecsdl.org/site/terms_use) unless CC License in place (see abstract).

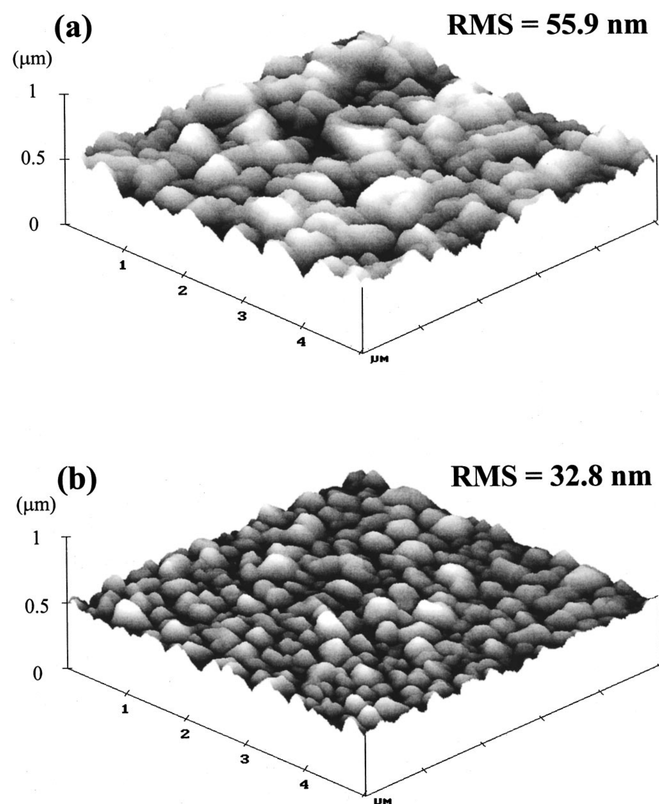


**Figure 11.** AFM images showing surface morphology of Cu films deposited on TaN substrates (a) without plasma treatment and (b) with Ar plasma treatment prior to Cu deposition.

The thicknesses of the Cu films with and without an Ar plasma substrate pretreatment are 348 and 408 nm, respectively, for a 10 min deposition at a substrate temperature of 160°C. The thinner Cu film on the Ar-plasma-treated TaN substrate is presumably due to the regular arrangement of smaller Cu grains, which in turn results in a denser microstructure and a smaller film thickness. The resistivity of the Cu film deposited on the Ar-plasma-treated TaN substrate was determined to be 3.40 μΩ cm, which is higher than that of the Cu film deposited on the substrate without the plasma treatment (2.30 μΩ cm), presumably due to the smaller Cu grains and thus a higher boundary density.

*Preferred orientation and postdeposition thermal annealing.*—The preferred orientation of Cu films is also affected by the Ar plasma treatment on the TaN substrate. Figure 12 shows the XRD spectra for Cu films deposited on TaN substrates with and without an Ar plasma treatment. It can be seen that the intensity peak ratio of Cu(111) to Cu(200) diffraction signals increased from 2.80 to 3.94 resulting from the Ar plasma treatment on the TaN substrate. With Ar plasma treatment, the smoother and thin amorphous-like TaN substrate surface enabled the migration of Cu-containing adspecies to the most stable site to forming a (111) preferential orientation because the (111) texture is the most stable configuration.[18,28]

Copper films deposited on the TaN substrate were thermally annealed at 400°C for 30 min in an $N_2$ ambient. Figure 13 shows the surface morphology of Cu films deposited on Ar-plasma-treated substrates before and after a thermal annealing. The thermally annealed Cu film reveals a closer contact between Cu grains, similar to those reported in the literature for CVD Cu films annealed in Ar and $Ar/H_2$ ambients.[31] Moreover, thermal annealing also resulted in decrease in film resistivity as well as increase in intensity peak ratio of Cu(111) to Cu(200) diffraction signals, as shown in Table II. The decrease in film resistivity is presumably due to the closer contact

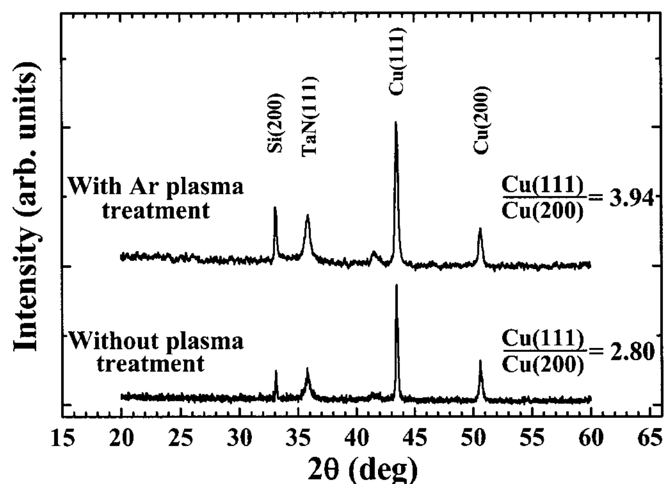


**Figure 12.** XRD spectra of Cu films deposited on TaN substrates with and without Ar plasma treatment prior to Cu deposition.

between the Cu grains. In addition, we presume that the Cu film deposited on the Ar-plasma-treated substrate possesses a uniform surface energy and little variation of film stress because of the better regular arrangement of Cu grains. As a result, thermal annealing would reduce the grain boundary and surface energy of the Cu film, resulting in the recrystallization of Cu grains to forming the most stable (111) texture.[18,32] On the other hand, Cu grains of different sizes are irregularly arranged for the Cu film deposited on the TaN substrate without a plasma treatment; thus, there is nonuniform surface energy and nonuniform films stress, and this nonuniformity would be reduced in order to reduce the total system energy during thermal annealing.[32] As a result, there is not enough driving force to recrystallize the Cu grains for the formation of the most stable (111) texture, and the improvement of the Cu(111)/Cu(200) intensity peak ratio was relatively moderate as compared with the Cu film deposited on the Ar-plasma-treated substrate. A similar observation was also reported for CVD Cu films thermally annealed at 450°C in Ar and $Ar/H_2$ ambients.[31] With regard to adhesion of Cu films, a Scotch tape pulling test was used to qualify the adhesion between the CVD Cu films and the TaN substrates. All samples with the Cu film deposited at 160°C and 150 mTorr, irrespective of substrate pretreatment by Ar plasma and/or post thermal annealing, passed the Scotch tape test. In summary, we conclude that the smoother TaN substrate surface with a higher surface energy resulting from the Ar plasma treatment, is responsible for the improvement of various Cu film properties.

## Conclusion

The CVD Cu films deposited on TaN substrate with and without an Ar plasma pretreatment and the effect of postdeposition thermal annealing were investigated. The Cu films deposited on the Ar-plasma-treated TaN substrate have a number of favorable properties over the films deposited on the TaN substrate without the plasma treatment. These include a smoother film surface, regular arrangement of Cu grains, and enhanced (111) preferential orientation. However, the Cu films deposited on the Ar-plasma-treated substrate have a higher electrical resistivity, presumably due to smaller grain size, and thus higher grain boundary density. Postdeposition thermal annealing resulted in the reduction of electrical resistivity and an increase of the Cu(111)/Cu(200) diffraction peak ratio. As a result of Ar plasma substrate pretreatment, we presume that the smoother and amorphous-like surface layer of the TaN substrate enhanced the formation of the most stable (111)-oriented Cu films, and that the higher substrate surface energy resulted in Cu films with a smoother surface and regularly shaped smaller grains. A combined process is proposed for the advantages of low resistivity and high (111)-

Downloaded on 2014-04-27 to IP 140.113.38.11 address. Redistribution subject to ECS terms of use (see ecsdl.org/site/terms_use) unless CC License in place (see abstract).

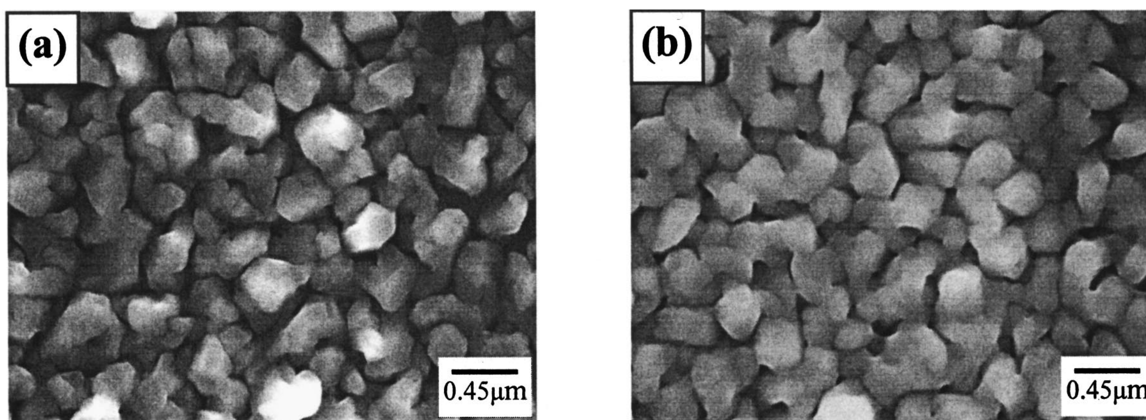


**Figure 13.** SEM micrographs showing surface morphology of Cu film deposited on TaN substrate with Ar plasma treatment prior to Cu deposition (a) as-deposited and (b) annealed at 400°C for 30 min in $N_2$ ambient.

**Table II. Effects of thermal annealing (400°C/30 min) on Cu films electrical resistivity and diffraction peak ratio of Cu(111)/Cu(200).**

| | Resisitvity (μΩ cm) | | Cu(111)/Cu(200) diffraction peak ratio | |
|---|---|---|---|---|
| Ar plasma treatment on TaN substrate | As-deposited | After anneal | As-deposited | After anneal |
| No | 2.30 | 2.15 | 2.80 | 3.10 |
| Yes | 3.40 | 2.10 | 3.94 | 5.14 |

oriented Cu film deposition. First, the TaN substrate is treated with Ar plasma prior to Cu film deposition, and second, the deposited Cu film is thermally annealed at an appropriate temperature (*e.g.*, 400°C) in an $N_2$ ambient.

*National Chiao-Tung University assisted in meeting the publication costs of this article.*

## References

1. A. Jain, A. V. Gelatos, T. T. Kodas, M. J. Hampden-Smith, R. Marsh, and C. J. Mogab, *Thin Solid Films,* **262**, 52 (1995).
2. C. K. Hu, B. Luther, F. B. Kaufman, J. Hummel, C. Uzoh, and D. J. Pearson, *Thin Solid Films,* **262**, 84 (1995).
3. A. Jain, T. T. Kodas, R. Jairath, and M. J. Hampden-Smith, *J. Vac. Sci. Technol. B,* **11**, 2107 (1993).
4. N. Awaya, H. Inokawa, E. Yamamoto, Y. Okazaki, M. Miyake, Y. Arita, and T. Kobayashi, *IEEE Trans. Electron Devices,* **ED-43**, 1206 (1996).
5. R. Kroger, M. Eizenberg, D. Cong, N. Yoshida, L. Y. Chen, S. Ramaswami, and D. Carl, *J. Electrochem. Soc.,* **146**, 3248 (1999).
6. C. H. Lee, K. H. Shen, T. K. Ku, C. H. Luo, C. C. Tso, H. W. Chou, and C. Hsia, *2000 IEEE International Interconnect Technology Conference*, p. 242, San Francisco, CA (2000).
7. B. Chin, P. Ding, B. Sun, T. Chiang, D. Angelo, I. Hashim, Z. Xu, S. Edelstein, and F. Chen, *Solid State Technol.,* **41**, 141 (1998).
8. R. L. Jackson, E. Broadbent, T. Cacouris, A. Harrus, M. Biberger, E. Patton, and T. Walsh, *Solid State Technol.,* **41**, 49 (1998).
9. Y. Shacham-Diamand and S. Lopatin, *Microelectron. Eng.,* **37/38**, 77 (1997).
10. P. Motte, M. Proust, J. Torres, Y. Gobil, Y. Morand, J. Palleau, R. Pantel, and M. Juhel, *Microelectron. Eng.,* **50**, 369 (2000).
11. N. I. Cho and Y. Sul, *Mater. Sci. Eng., B,* **72**, 184 (2000).
12. S. Voss, S. Gandikota, L. Y. Chen, R. Tao, D. Cong, A. Duboust, N. Yoshida, and S. Ramaswami, *Microelectron. Eng.,* **50**, 501 (2000).
13. R. Kroger, M. Eizenberg, D. Cong, N. Yoshida, L. Y. Chen, S. Ramaswami, and D. Carl, *Microelectron. Eng.,* **50**, 375 (2000).
14. M. T. Wang, Y. C. Lin, and M. C. Chen, *J. Electrochem. Soc.,* **145**, 2538 (1998).
15. D. H. Kim, R. H. J. Wentorf, and W. N. Gill, *J. Appl. Phys.,* **74**, 5164 (1993).
16. K. Hanaoka, H. Ohnishi, and K. Tachibana, *Jpn. J. Appl. Phys., Part 1,* **34**, 2430 (1995).
17. Y. S. Kim, D. Jung, and S. K. Min, *Thin Solid Films,* **349**, 36 (1999).
18. K. Kamoshida and Y. Ito, *J. Vac. Sci. Technol. B,* **15**, 961 (1997).
19. J. A. T. Norman, B. A. Mutamore, P. N. Dyer, D. A. Roberts, and A. K. Hochberg, *J. Phys. IV,* **1**, C2-271 (1991).
20. J. C. Chiou, Y. J. Chen, and M. C. Chen, *J. Electron. Mater.,* **23**, 383 (1994).
21. T. Nguyen, L. J. Charneski, and S. T. Hsu, *J. Electrochem. Soc.,* **144**, 2829 (1997).
22. A. Jain, K. M. Chi, T. T. Kodas, and M. J. Hampden-Smith, *J. Electrochem. Soc.,* **140**, 1434 (1993).
23. Y. K. Chae, Y. Shimogaki, and H. Komiyama, *J. Electrochem. Soc.,* **145**, 4226 (1998).
24. S. S. Yoon, J. S. Min, and J. S. Chun, *J. Mater. Sci.,* **30**, 2029 (1995).
25. P. J. Lin and M. C. Chen, *Jpn. J. Appl. Phys., Part 1,* **38**, 4863 (1999).
26. M. Avinun, W. D. Kaplan, M. Eizenberg, T. Guo, and R. Mosely, *Solid-State Electron.,* **43**, 1011 (1999).
27. R. J. Stokes and D. F. Evans, *Fundamentals of Interfacial Engineering*, p. 59, Wiley-VCH, Inc., New York (1997).
28. H. Toyoda, T. Kawanoue, S. Ito, M. Hasunuma, and H. Kaneko, in *Stress-Induced Phenomena in Metallization, Third International Workshop*, Palo Alto, CA, USA, June 1995, P. S. Ho, J. Bravman, C. Y. Li, and J. Sanchez, Editors, No. 373, p. 169, American Institute of Physics Conference Proceedings, New York (1996).
29. A. Weber, U. Bringmann, K. Schiffmann, and C. P. Klages, *Mater. Res. Soc. Symp. Proc.,* **282**, 311 (1993).
30. J. H. Lee, J. H. Lee, K. J. Hwang, J. Y. Kim, C. G. Suk, and S. Y. Choi, *Thin Solid Films,* **375**, 132 (2000).
31. S. K. Rha, W. J. Lee, S. Y. Lee, D. W. Kim, C. O. Park, and S. S. Chun, *Jpn. J. Appl. Phys., Part 1,* **35**, 5781 (1996).
32. C. V. Thompson and R. Carel, *Mater. Sci. Eng.,* **B32**, 211 (1995).

Downloaded on 2014-04-27 to IP 140.113.38.11 address. Redistribution subject to ECS terms of use (see ecsdl.org/site/terms_use) unless CC License in place (see abstract).